GENERAL ENDOCRINOLOGY

Elevated Mechanical Loading When Young Provides Lifelong Benefits to Cortical Bone Properties in Female Rats Independent of a Surgically Induced Menopause

Stuart J. Warden, Matthew R. Galley, Andrea L. Hurd, Joseph M. Wallace, Maxime A. Gallant, Jeffrey S. Richard, and Lydia A. George

Center for Translational Musculoskeletal Research (S.J.W., M.R.G., A.L.H.) and Department of Physical Therapy (S.J.W., J.S.R., L.A.G.), School of Health and Rehabilitation Sciences, and Department of Anatomy and Cell Biology (M.A.G.), School of Medicine, Indiana University; and Department of Biomedical Engineering (J.M.W.), Purdue School of Engineering and Technology, Indiana University-Purdue University Indianapolis, Indianapolis, Indiana 46202

Exercise that mechanically loads the skeleton is advocated when young to enhance lifelong bone health. Whether the skeletal benefits of elevated loading when young persist into adulthood and after menopause are important questions. This study investigated the influence of a surgically induced menopause in female Sprague-Dawley rats on the lifelong maintenance of the cortical bone benefits of skeletal loading when young. Animals had their right forearm extrinsically loaded 3 d/wk between 4 and 10 weeks of age using the forearm axial compression loading model. Left forearms were internal controls and not loaded. Animals were subsequently detrained (restricted to cage activities) for 94 weeks (until age 2 years), with ovariectomy (OVX) or sham-OVX surgery being performed at 24 weeks of age. Loading enhanced midshaft ulna cortical bone mass, structure, and estimated strength. These benefits persisted lifelong and contributed to loaded ulnas having greater strength after detraining. Loading also had effects on cortical bone quality. The benefits of loading when young were not influenced by a surgically induced menopause because there were no interactions between loading and surgery. However, OVX had independent effects on cortical bone mass, structure, and estimated strength at early postsurgery time points (up to age 58 weeks) and bone quality measures. These data indicate skeletal loading when young had lifelong benefits on cortical bone properties that persisted independent of a surgically induced menopause. This suggests that skeletal loading associated with exercise when young may provide lifelong antifracture benefits by priming the skeleton to offset the cortical bone changes associated with aging and menopause. (*Endocrinology* 154: 3178–3187, 2013)

Exercise that mechanically loads the skeleton provides a potent stimulus to alter bone mass, structure, and strength (1). The young skeleton is generally accepted as being most responsive to the mechanical loads engendered during exercise, with the skeletal benefit of a lifetime of exercise occurring mainly during the years of skeletal development (2, 3). Because the skeleton is most at risk of failure during aging, the question is raised as to whether the skeletal benefits of exercise-induced mechanical loading when young persist into late adulthood where they may be advantageous in reducing fracture risk (4, 5).

Elevated mechanical loading of the skeleton via exercise during growth is advocated as a means of achieving a higher peak bone mass to prime the skeleton to offset the bone loss associated with aging (6, 7). Numerous animal and clinical studies have demonstrated cessation of exer-

Abbreviations: AFM, atomic force microscopy; BMC, bone mineral content; μCT, micro-computed tomography; Ct.Ar, cortical area; Ct.Th, cortical thickness; I_{MIN}, minimum second moment of area; Me.Ar, medullary area; OVX, ovariectomy; pQCT, peripheral quantitative computed tomography; RPI, reference point indentation; Tt.Ar, total area; vBMD, volumetric bone mineral density.

cise is associated with partial maintenance of the bone mass benefits of elevated mechanical loading during growth (8-10); however, these mass benefits appear to diminish over time and may not last lifelong (11–16). In contrast, mechanisms exist for loading-induced bone structural changes generated when young to last lifelong.

Exercise-induced skeletal loading during growth induces a disproportionate increase in bone mechanical properties without a substantial increase in bone mass (17, 18). This occurs as elevated mechanical loading during growth deposits new bone on the outer periosteal surface to increase bone size, with bone mechanical properties being proportional to the fourth power of the bone radius. Because bone loss during aging occurs primarily on the endocortical and not periosteal surface (19), the discordant surface effects of mechanical loading and aging potentially enables the structural benefits of exercise-induced loading during growth to persist long-term and have lasting benefits on bone strength.

We previously demonstrated that elevated mechanical loading during a period of rapid growth in estrogen-replete rats had lifelong benefits on cortical bone structure and strength, independent of the maintenance of bone mass benefits (16). An important translational question is whether the skeletal benefits of elevated mechanical loading during growth persist with subsequent estrogen depletion. This would represent the clinical scenario of exercise-induced mechanical loading during growth followed by menopause later in life. Umemura et al (20) preliminarily investigated this question by exercising 12-week-old ovariectomized rats for 8 weeks and following them for 6 months after exercise cessation. Data suggested no impact of estrogen removal on the maintenance of the bone mass and strength benefits of exercise; however, animals were not followed lifelong.

The aim of the current study was to investigate the influence of a surgically induced menopause in female rats on the lifelong maintenance of mechanical loading-induced cortical bone benefits generated when young. Unilateral skeletal loading was introduced extrinsically using the forearm axial compression loading model (21), whereas surgically induced menopause was achieved by ovariectomy (OVX).

Materials and Methods

Animals

Forty virgin female Sprague-Dawley rats (Harlan Sprague-Dawley, Inc, Indianapolis, Indiana) were acclimatized until 4 weeks of age before experimentation. All procedures were performed with previous approval of the Institutional Animal Care and Use Committee of Indiana University.

Mechanical loading

The right forearm of each animal was mechanically loaded beginning at 4 weeks of age using the forearm axial compression loading model (21). Loading was performed using an electromechanical actuator (ElectroForce 3200; Bose Corporation, Eden Praire, Minnesota) with the animal under inhalation anesthesia. The initial peak load was 8.5 N, which elicited a compressive strain (ϵ) of approximately 3500 $\mu\epsilon$ on the medial surface of the ulna midshaft, as determined in a previous strain gauge experiment (16). Loads were introduced using a 2-Hz haversine waveform for 360 cycles/d, 3 d/wk for 6 weeks. The peak load was increased weekly in proportion to the increase in body mass to counter the increase in bone size associated with rapid growth in young animals and consequent decrease in strain per given load. The peak load during the final loading session was 19.0 N. Left ulnas served as internal controls and were not loaded. Animals were 10 weeks of age by the end of the loading program at which time they began 94 weeks of detraining. Normal cage activity was allowed between loading sessions and throughout detraining.

Surgery

At 24 weeks of age (after 14 weeks of detraining), animals were randomly divided into 2 surgery groups: OVX and sham-OVX. Surgeries were performed under inhalation anesthesia with the delay between completion of the loading program and surgery used to replicate the clinical scenario of exercise-induced mechanical loading when young followed by menopause later in life. Animals in the OVX group had both ovaries removed via a dorsal approach, as previously described (22). Animals in the sham-OVX group had their ovaries exteriorized but not removed.

In vivo assessment of bone status

Adaptation to loading and bone status during detraining were determined in vivo by assessing the right (loaded) and left (nonloaded) forearms using an XCT Research SA+ peripheral quantitative computed tomography (pQCT) machine (Stratec Medizintechnik GmbH, Pforzheim, Germany). pQCT was performed under inhalation anesthesia before (age 4 weeks) and at the completion of the loading program (age 10 weeks), and at frequent intervals (every 3–12 weeks) during detraining. A transverse midshaft scan was taken of each ulna using a 70-μm voxel size after performance of a localizing scout scan. Analyses were restricted to cortical bone, with the bone edge detected using contour mode 1 (threshold = 400 mg/cm^3). Volumetric bone mineral density (vBMD) (mg/cm^3), bone mineral content (BMC) (mg/mm), and cortical area (Ct.Ar) (mm^2) were recorded, and the minimum second moment of area (I_{MIN}) (mm^4) was derived. I_{MIN} refers to the distribution of bone mineral around the plane of least bending rigidity and provides an indirect measure of ulna mechanical properties to axial compression (16, 17).

Ex vivo assessment of bone status

Animals were euthanized after 94 weeks detraining (age 2 years), and the loaded and nonloaded ulnas were dissected and stored in ethanol. A desktop microcomputed tomography (μCT)
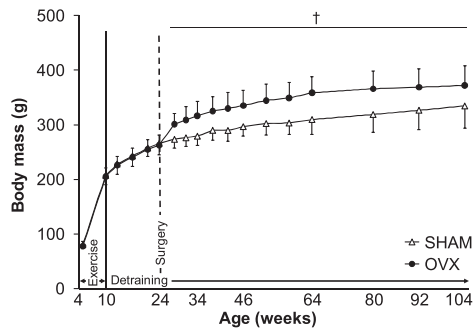
Figure 1. Body mass and the effect of surgical intervention on body mass at select time points during the study. There were no group differences in body mass before surgical intervention (all $P > .55$, unpaired t test). †, OVX (n = 18) had 10% to 15% greater body mass after surgery and throughout aging compared with sham-OVX (n = 16) (all $P < .001$, unpaired t test).

machine (SkyScan 1172 high-resolution μCT; SkyScan, Kontich, Belgium) scanning with an 11.8-μm isotropic voxel size was used to obtain tomographic slices along the bone length. Images were imported into ImageJ version 1.45s (National Institutes of Health, Bethesda, Maryland), and analyzed using the plugin BoneJ version 1.3.3 (23) and customized macros to acquire total area (Tt.Ar) (mm²), Ct.Ar (mm²), medullary area (Me.Ar) (mm²), cortical thickness (Ct.Th) (mm), and I_{MIN} (mm⁴) at increments of 5% of bone length.

Ex vivo assessment of bone mechanical properties

Loaded and nonloaded ulna pairs from 10 OVX and 10 sham-OVX animals were tested in axial compression, as previously described (16, 17). Bones were rehydrated in saline and fixed between 2 cups on an electromechanical actuator (ElectroForce 3200; Bose). Loading to failure was performed using monotonic compression at 2 mm/s during which force and displacement measures were collected at 100 Hz. From the force versus displacement curves, ultimate force (N), yield force (N), stiffness (N/mm), postyield energy (mJ), and postyield displacement (mm) were derived. The yield point was defined using a 0.015-mm offset parallel to the stiffness (24).

Ex vivo assessment of bone gain during detraining

An ip injection of calcein (7 mg/kg; Sigma Chemical Co, St. Louis, Missouri) and alizarin (30 mg/kg; Sigma) was administered at the completion of the loading program (age 10 weeks) and at the time of surgery (age 24 weeks), respectively. Bone segments from ulna pairs of 6 OVX and 6 sham-OVX animals were embedded in methylmethacrylate, and transverse thick (50 μm) sections were removed at 40% of ulna length from the distal end, as previously described (16). Sections were imaged on a Leica DMI6000 inverted microscope (Leica Mikrosysteme Vertrieb GmbH, Wetzlar, Germany) and analyzed with Image-Pro Plus (version 7.0; Media Cybernetics, Inc, Bethesda, Maryland). Gain in bone area during detraining (mm²) was measured as the area of bone between the intracortical calcein label and perios-
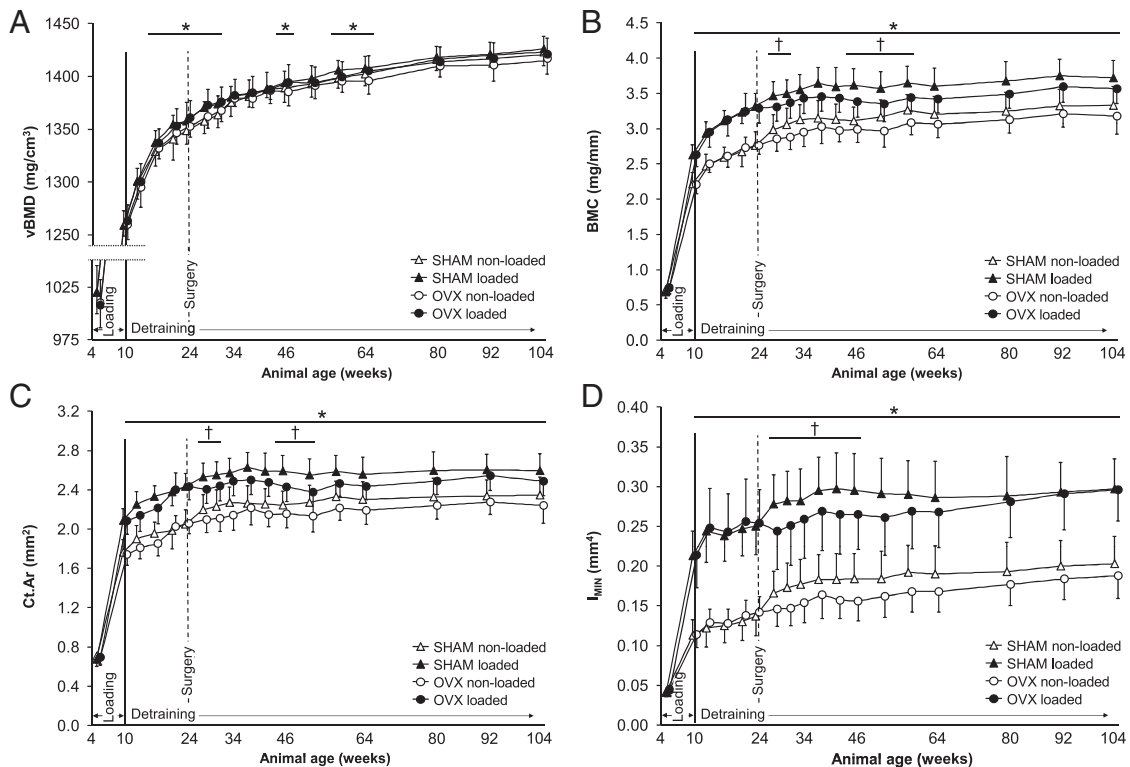

Figure 2. Mechanical loading when young had lifelong benefits on cortical bone properties independent of a surgically induced menopause (sham-OVX, n = 16; OVX, n = 18). Graphs show the effect of loading and surgery at select time points on in vivo assessed ulna midshaft: A, vBMD; B, BMC; C, Ct.Ar; D, I_{MIN}. There were no statistical interactions between loading and surgery at any time point (all $P > .31$), indicating surgery did not influence the maintenance of the skeletal effects of loading during detraining. Data represent mean ± SD. *, Significant independent effect for loading at specific time point, with values in loaded ulnas (filled markers) being greater than in nonloaded ulnas (open markers). †, Significant independent effect for surgery at specific time point, with values in sham-OVX (triangles) being greater than in OVX (circles).

teal bone perimeter. This bone area was subsequently subdivided into bone gained between loading completion and surgery (calcein to alizarin label) and postsurgery bone gain (alizarin label to periosteal bone perimeter).

Ex vivo assessment of bone material properties

Bone material properties were assessed in subsets of specimens using reference point indentation (RPI) and atomic force microscopy (AFM) and via determination of ash content. RPI and AFM were performed in separate ulna pairs from 4 OVX and 4 sham-OVX animals. Measurements were performed on the medial surface of the ulna diaphysis at a distance of 40% of ulna length from its distal end. This location corresponds with the area of maximal adaptation resulting from forearm axial compression loading (16, 17).

RPI was performed with a Bone Probe 3 using a Biodent Hfc RPI instrument (Active Life Scientific, Inc, Santa Barbara, California), as previously described (25, 26). The probe applied 10 indentation cycles at 2 Hz with a maximum force of 10 N. The first cycle unloading slope (N/μm) and indentation distance increase over the entire set of cycles (μm) were recorded as indicators of intrinsic stiffness and toughness, respectively (25, 26). Measurements were performed in triplicate and averaged, with repeat measures performed 1 mm apart.

AFM was performed with a ScanAsyst Fluid+ probe operating in peak force tapping mode on a Catalyst AFM instrument (Bruker AXS, Inc, Madison, Wisconsin). A flat surface of bone was created just below the medial periosteal surface using a 3-μm polycrystalline water-based diamond suspension (Buehler Ltd, Lake Bluff, Illinois). Extrafibrillar surface mineral was removed and the underlying collagen fibrils exposed via 4 cycles of demineralization in 0.5M EDTA (pH 8.0) for 20 minutes followed by sonication in ultrapure water for 5 minutes. Images were initially acquired using 25 $\times$ 25 μm scans at 3 or more locations within each sample to find sites for closer inspection. Scan size was subsequently decreased to a final size of 3.5 $\times$ 3.5 μm, and peak force error images were analyzed to investigate the D-periodic spacing of individual collagen fibrils using a 2-dimensional fast Fourier transform, as previously described (27-30).

Ash content was determined in ulna pairs from 6 OVX and 6 sham-OVX animals by placing bone segments in a muffle furnace. The furnace was set at 100°C for 24 hours to remove water, followed by 800°C for 24 hours to remove organic material. Bone segments were weighed after the first and second 24-hour periods to obtain dry and ash weight, respectively. Percent ash content was calculated as (ash weight/dry weight) $\times$ 100.

Statistical analyses

Analyses were performed with IBM SPSS Statistics (version 20.0; SPSS Inc, Chicago, Illinois), and were 2-tailed with a level of significance set at 0.05. Two-way, 1-repeated-measure analyses of covariance (ANCOVA) were used to assess in vivo bone outcomes (except vBMD), ex vivo bone structural properties at 5% increments of bone length, and bone gain during detraining and mechanical properties, with loading (loaded vs nonloaded) and surgical (sham-OVX vs OVX) groups being the within- and between-animal independent variables, respectively. Body mass was used as the covariate. Bone material properties (including in vivo vBMD) were similarly assessed with 2-way, 1-repeated-
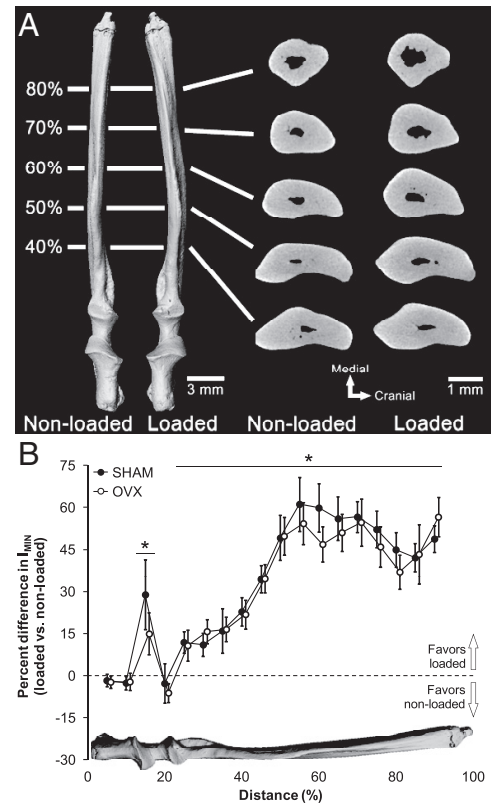

Figure 3. Loading-induced changes in estimated cortical bone mechanical properties were maintained after 94 weeks of detraining (age 104 weeks), localized in the distal portions of the bone, and not influenced by a surgically induced menopause. A, μCT obtained cranial (images on left) and cross-sectional (images on right) views of nonloaded and loaded ulnas from a representative animal. Note the substantially increased mediolateral diameter of the diaphysis in the loaded ulna, particularly in the midshaft and distal regions. B, Mean percent differences in I_{MIN} between loaded and nonloaded ulnas in OVX (n = 18) and sham-OVX (n = 16) animals at 5% increments along the bone length measured ex vivo using μCT. *, Loading effects were predominantly induced and maintained in the distal portions of the bone, as evident by mean percent differences and their 95% confidence intervals (error bars) being greater than 0% (all $P < .05$). There was no effect of surgery (sham-OVX vs OVX) on percent difference in I_{MIN} between loaded and nonloaded ulnas (all $P = .19–.92$).

measure ANOVA. Main effects for loading and surgical group were explored in the advent of a nonsignificant analysis of covariance (ANCOVA)/ANOVA interaction. The effect of surgery (sham-OVX vs OVX) on the maintenance of exercise effects on I_{MIN} at 5% increments of bone length was assessed using unpaired t tests on the mean percent differences between loaded and nonloaded ulnas. To investigate differences in the distribution of AFM-derived collagen fibril morphology between groups, cumulative distribution functions were compared using Kolmogorov-Smirnov tests.

Results

Animal characteristics

Forty-five percent of animals (18 of 40) developed 1 or more benign mammary tumors (fibroadenomas) during
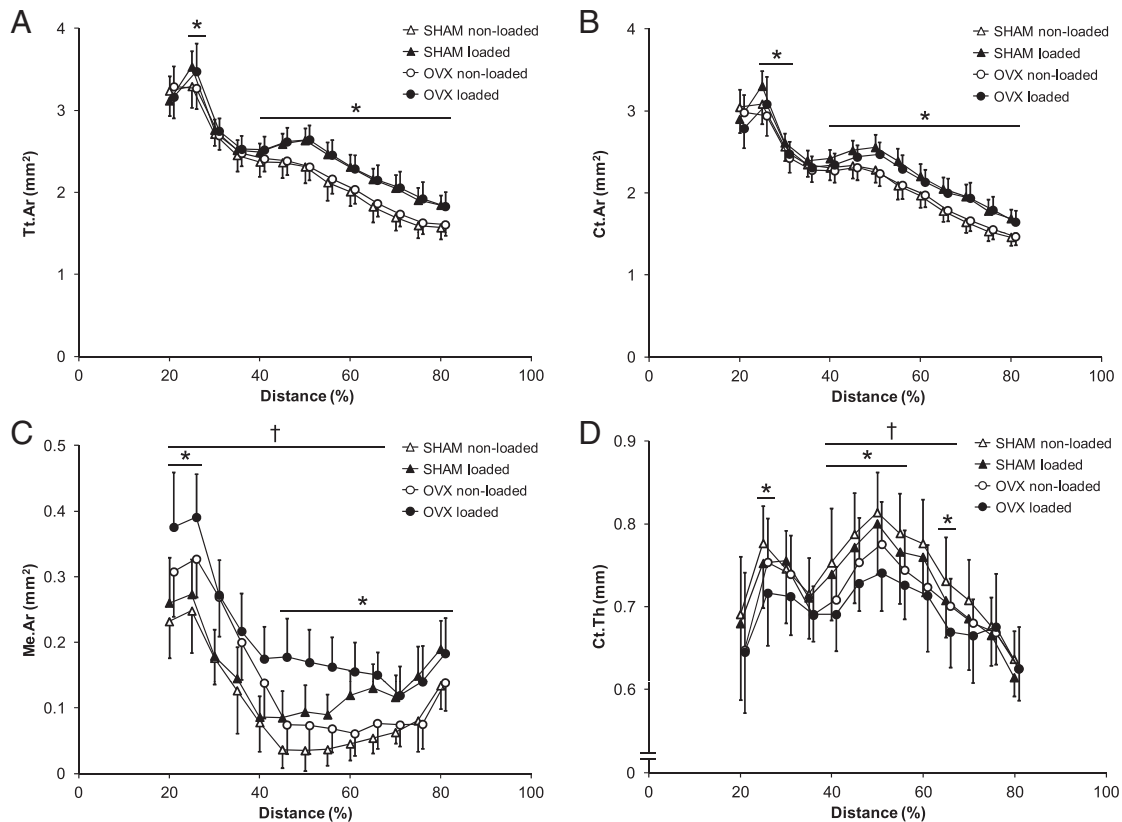
Figure 4. Loading-induced changes in cortical bone structure at 5% increments along the bone length were present after 94 weeks of detraining (age 104 weeks) and not influenced by a surgically induced menopause (sham-OVX, n = 16; OVX, n = 18). There were no statistical interactions between loading and surgery at any location (all $P > .08$), indicating surgery did not influence the skeletal effects of loading during detraining. Loaded ulnas (filled markers) had increased Tt.Ar (A), Ct.Ar (B) and Me.Ar (C), and decreased C.Th (D) at numerous locations along the bone length relative to nonloaded ulnas (open markers). OVX (circles) had increased Me.Ar and decreased Ct.Th relative to sham-OVX (triangles). Data represent mean ± SD. *, Significant independent effect for loading at specific bone increment. †, Significant independent effect for surgery at specific bone increment.

aging. OVX (4 of 20) developed fewer tumors than sham-OVX (14 of 20) ($P < .01$, Fisher's exact test), consistent with previous reports of the protective effects of OVX (31, 32). Palpable tumors were removed by surgical excision. Six animals (sham-OVX, n = 4; OVX, n = 2) died before completion of the 94-week detraining period. Two animals died as a result of anesthetic complications, whereas 4 others died of unknown/natural causes. Data from these 6 animals were excluded from analyses. Body mass differed between sham-OVX and OVX after surgery (all $P < .05$, unpaired t test) (Figure 1).

Effects of loading and surgery on in vivo cortical bone properties across the lifespan

In vivo bone measures at select time points throughout the study are shown in Figure 2. There were no group differences in any measure at the commencement of loading (age 4 weeks) (all $P > .20$). At the completion of loading (age 10 weeks), loaded forearms had greater midshaft ulna BMC, Ct.Ar, and I_{MIN} (all $P < .001$; Figure 2, B–D). The largest exercise effect was on I_{MIN}, which was 88% greater in loaded forearms compared with nonloaded

forearms. There was no effect of loading on midshaft ulna vBMD when assessed at the completion of loading (age 10 weeks); however, loaded forearms had elevated vBMD beginning at 7 weeks detraining (age 17 weeks) and at varying time points thereafter up to 64 weeks of age (Figure 2A).

There were no differences between surgical groups on any measure before surgery (all $P > .20$) and no statistical interactions between loading and surgery after surgical intervention (all $P > .31$). The latter finding indicates surgery did not influence the maintenance of the skeletal effects of loading during detraining. There was no effect of surgery on vBMD at any time (Figure 2A); however, OVX had a negative main effect on BMC, Ct.Ar, and I_{MIN} at varying times during the initial weeks after surgery (up to age 58 weeks) (Figures 2, B–D). There was no effect of surgery on any in vivo measure beyond 58 weeks of age (all $P \geq .08$).

Loading completed when young had persistent beneficial effects on BMC, Ct.Ar, and I_{MIN} at all time points during detraining (all $P < .05$; Figure 2, B–D). There was

no convergence between BMC, Ct.Ar, and I_{MIN} values obtained in loaded and nonloaded ulnas during detraining. For instance, the absolute difference in I_{MIN} between loaded and nonloaded ulnas at the completion of loading ($0.098 \pm 0.037\,mm^4$) and after detraining ($0.103 \pm 0.036\,mm^4$) did not differ ($P = .83$, paired t test).

Effects of loading and surgery on ex vivo cortical bone properties after detraining

Ulnas from loaded forearms were qualitatively and quantitatively larger than ulnas from nonloaded forearms after detraining (Figure 3). Loading benefits were predominantly induced and maintained in the distal portions of the bone (Figure 3B). There was no effect of surgery on the percent difference in I_{MIN} between loaded and nonloaded ulnas (all $P = .19$–$.92$) indicating an absence of a surgery effect on the maintenance of the skeletal effects of loading during detraining.

There were no statistical interactions between loading and surgery on bone structural properties assessed ex vivo after detraining (all $P > .08$) (Figure 4). Loaded ulnas had increased Me.Ar (Figure 4C) and decreased Ct.Th (Figure 4D) at various locations after detraining; however, Tt.Ar (Figure 4A) and Ct.Ar (Figure 4B) were increased relative to nonloaded ulnas (all $P < .05$). OVX increased Me.Ar (Figure 4C) and decreased Ct.Th (Figure 4D) at various diaphyseal locations (all $P < .05$) relative to sham-OVX, but there was no influence of surgery on Tt.Ar or Ct.Ar (all $P > .05$).

Gain in bone area during detraining was equivalent between loaded and nonloaded ulnas and between sham-OVX and OVX animals when assessed histomorphometrically (all $P > .21$, Figure 5). Similarly, there were no group differences on bone gained between loading completion and surgery, or bone gained after surgery (all $P > .35$, data not shown).

Effects of loading and surgery on bone mechanical properties after detraining

There were no statistical interactions between loading and surgery (all $P = .42$–$.99$) or effect of surgery (all $P = .08$–$.83$) on any mechanical property (Figure 6). Loaded ulnas had 23.3% and 28.5% greater ultimate force and stiffness than nonloaded ulnas, respectively (all $P < .001$; Figure 6, A–C). Yield force was 27.5% higher in loaded versus nonloaded ulnas ($P = .04$, data not shown); however, loaded ulnas absorbed 19.9% less postyield energy ($P = .04$; Figure 6D) and had 36.8% less postyield displacement than nonloaded ulnas ($P < .001$, data not shown). Loaded ulnas broke in more than 1 place (17 of 20 ulnas) with greater frequency than nonloaded ulnas (9 of 20 ulnas) ($P = .02$, Fisher's exact test).
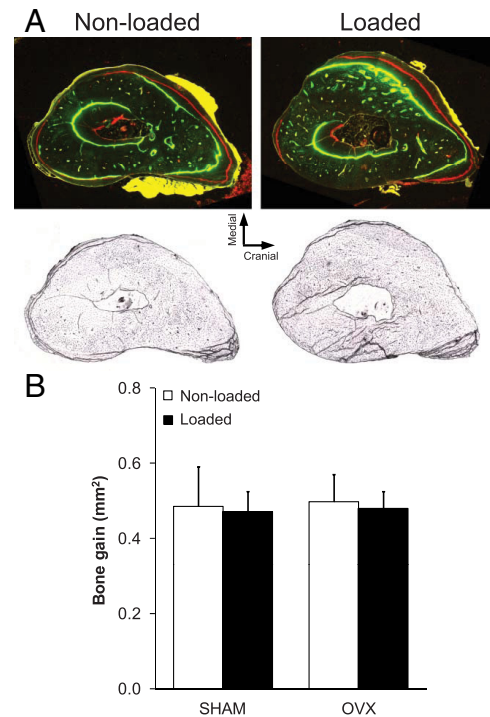

Figure 5. A, Histological images of nonloaded and loaded ulnas from a representative animal under fluorescent (top row) and white (bottom row) light. Bone area gain during detraining was measured under fluorescent light as the bone area between the calcein (green) label administered at the completion of the loading program (age 10 weeks) and the periosteal bone perimeter (age 104 weeks). The alizarin (red) label indicates bone size and shape at the time of surgery (age 24 weeks). Under white light, note the increased cortical area of the loaded ulna and, in particular, the greater distribution of bone in the mediolateral plane. This plane approximates the plane of least bending resistance (I_{MIN}) in the rat ulna. B, Gain in bone area during detraining was equivalent between loaded and nonloaded ulnas and between sham-OVX (n = 6) and OVX (n = 6) animals (all $P > .21$). These data indicate there was no catch-up phenomenon during detraining whereby nonloaded bones caught up the superior bone area of loaded bones.

Effects of loading and surgery on bone material properties after detraining

There were no statistical interactions between loading and surgery on bone material properties (all $P = .66$–$.89$). Loaded ulnas had 4.8% and 0.7% greater first cycle unloading slope and ash content, respectively (all $P < .05$, Figure 7, A and B). There was no effect of loading on indentation distance increase ($P = .38$, data not shown), or distribution of collagen D-periodic spacing in sham-OVX ($P = .13$, Figure 7C) or OVX ($P = .06$, Figure 7D) animals. OVX caused a 6.8% decrease in first cycle unloading slope ($P < .05$, Figure 6A) and a shift toward lower collagen D-periodic spacing ($P = .04$, Figure 7E).

Discussion

This study found elevated mechanical loading of the skeleton completed when young had lasting benefits on cor-
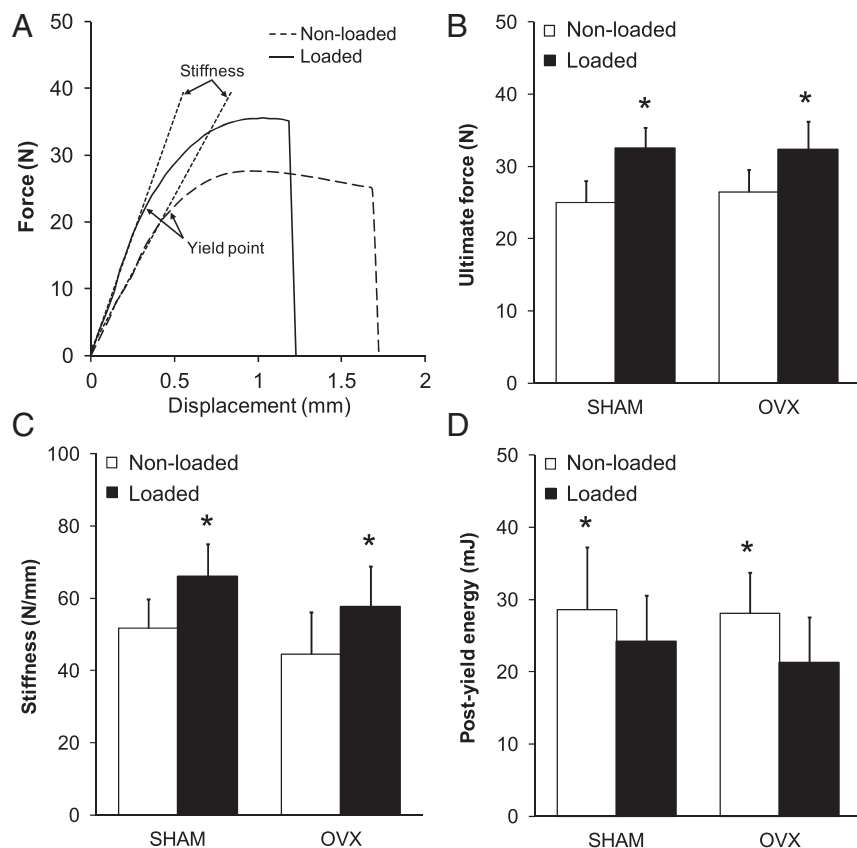
Figure 6. Elevated mechanical loading completed when young had lifelong benefits on bone strength independent of a surgically induced menopause (sham-OVX, n = 10; OVX, n = 10). A, Representative force vs displacement curves for a pair of loaded and nonloaded ulnas from a sham-OVX animal after detraining (curves from a single surgery group are shown for clarity and because there were no surgery effects on mechanical properties). There were no statistical interactions between loading and surgery or independent effect of surgery on any measure (all $P > .31$); however, loaded ulnas had greater ultimate force (B) (peak of the curve on the y-axis in A); greater stiffness (C) (slope of the linear portion of the curve in A), and less postyield energy (D) (area under curve between yield point and failure in A) than nonloaded ulnas (*, $P < .001$ for loading independent effect).

had independent negative effects on cortical bone properties, decreasing cortical bone mass and area at early time points after surgery (up to age 58 weeks) and increasing Me.Ar, decreasing Ct.Th, and altering bone quality when assessed after detraining (at age 2 years). These cumulative data suggest elevated skeletal loading when young provided lifelong benefits to cortical bone properties that were not influenced by menopause, with loading essentially priming the skeleton to offset the cortical bone changes associated with OVX.

The observation that elevated skeletal loading completed when young provided lifelong benefit is in general agreement with our previous work (16). In our previous study, we used the forearm axial compression loading model to demonstrate skeletal loading when young had lifelong benefits on bone structure and strength but not bone mass. The current data support these findings, with the exception that there was also lifelong maintenance of the bone mass benefits of loading. A possible reason for the contrasting bone mass finding between our 2 studies may relate to the use of different imaging modalities, with bone mass in our previous and current studies being assessed by dual-energy x-ray absorptiometry and pQCT, respectively. Dual-energy x-ray absorptiometry provides a useful measure of generalized bone health but is limited in revealing the site-specific skeletal benefits of exercise because of its planar nature and low spatial resolution (34). In contrast, pQCT provides relatively high-resolution tomographic images to provide more localized measures at site-specific regions along the bone length.

Surgically induced menopause did not influence the lifelong maintenance of the skeletal benefits of loading because there were no statistical interactions between the loading and surgical intervention groups. The absence of an interaction between the interventions indicates that the skeletal benefits of loading were maintained equally in sham-OVX and OVX animals. This observation supports the findings of Umemura et al (20) who showed no effect of OVX on the maintenance of jump training-induced changes in tibial bone properties in rats exercised for 8
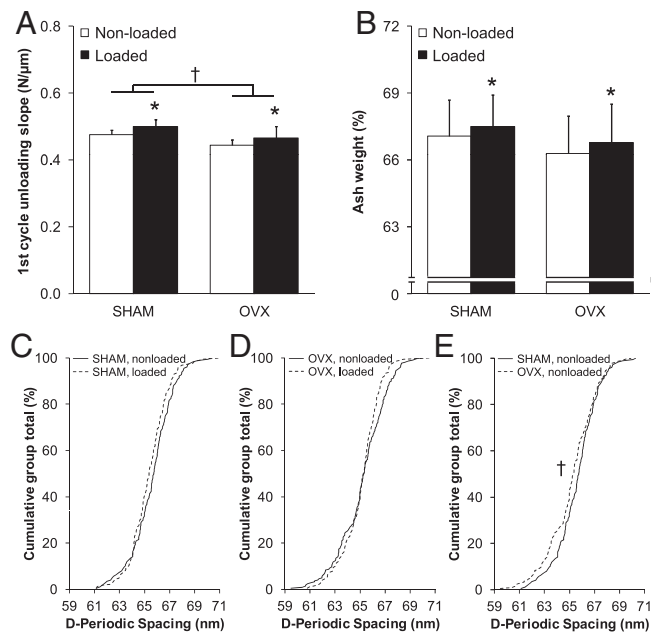
tical bone properties that persisted independent of a surgically induced menopause. Skeletal loading using the forearm axial compression loading model for 6 weeks when young increased cortical bone mass, altered bone structure, and enhanced bone strength of the ulna in loaded forearms relative to contralateral nonloaded forearms. These exercise-induced cortical bone benefits persisted despite animals subsequently being restricted to home-cage physical activities for a detraining period of 94 weeks (until 2 years of age). Because only 60% of female Sprague-Dawley rats in captivity typically survive beyond 2 years of age (33), the animals were senescent by the end of the study such that the cortical bone benefits of elevated skeletal loading when young were maintained virtually lifelong. The lifelong maintenance of loading benefits was not influenced by an OVX-induced menopause, as evident by the absence of statistical interactions between the loading and surgery groups. However, OVX

Figure 7. Elevated mechanical loading completed when young and a surgically induced menopause during aging had independent lifelong effects on bone quality. Loaded ulnas had greater intrinsic stiffness (A) (as indicated by first cycle unloading slope) and greater mineralization (B) (as indicated by ash weight) (*, $P < .05$ for loading effect). There was no effect of loading on the distribution of collagen D-periodic spacing in either sham-OVX (C) or OVX (D) animals. OVX animals (n = 4) had reduced intrinsic stiffness (A) and a shift toward lower collagen D-periodic spacing (E) compared with sham-OVX animals (n = 4) (†, $P < .05$ for surgery effect).

weeks and subsequently detrained for 6 months (until age 11 months). The data from the current study further the body of evidence by studying animals lifelong (until age 2 years), performing within-animal comparisons, and performing comprehensive measures of bone mass, structure, strength and quality.

Surgically induced menopause had an independent effect on cortical bone properties. OVX in rodents generates a cortical bone modeling drift such that there is endosteal resorption and periosteal apposition (35-38), as occurs postmenopause in humans (19). Because more bone is removed endosteally than formed periosteally after OVX, the net result is a reduction in bone mass and cortical bone area. Such bone mass and cortical bone area changes were observed in the current study at early time points after surgery (up to age 58 weeks); however, they did not statistically persist lifelong (as assessed in vivo using pQCT and ex vivo using μCT). OVX animals had increased μCT-derived Me.Ar at the completion of detraining, but the absolute increase in medullary area (suggestive of elevated endosteal resorption) was small such that it had minimal influence on cortical bone quantity and other structural measures. However, OVX did cause a long-term change in bone quality decreasing intrinsic stiffness

(decrease in first cycle unloading slope) and changing collagen fibril morphology (shift toward lower D-periodic spacing), consistent with previous studies (29, 39, 40).

The maintenance of loading-induced changes in cortical bone mass and structure had functional benefits. In particular, ulnas from loaded forearms had greater ultimate force, yield force, and stiffness than ulnas from non-loaded forearms. These findings suggest exercise that elevates skeletal loading when young could have lifelong antifracture benefits independent of estrogen status. However, a potential caveat is the negative effect of loading completed when young on bone quality. Ulna adaptation in response to axial compression loading in rats typically enhances postyield properties (17), but when loaded was coupled with detraining in the current study, it reduced both postyield displacement and energy. Postyield properties indicate ductility, with reductions in postyield displacement and energy indicating increased brittleness. Increased brittleness of loaded ulnas was confirmed by their greater frequency of breaking in more than 1 place than nonloaded ulnas. Exploring potential mechanisms for the increase in brittleness, loaded ulnas were found to have greater tissue mineralization (as indicated by increased whole-bone ash content) and increased intrinsic stiffness.

The functional consequence of increased brittleness in loaded ulnas may be that exercise-induced mechanical loading during growth followed by detraining may create bones more susceptible to developing and propagating load-related damage. We tested this in our previous study by assessing the fatigue life of previously loaded and nonloaded ulnas (16). Ulnas were cyclically loaded until fatigue failure at a constant load, as opposed to strain, because the former approximates the function requirements of the bone. Loaded ulnas had substantially greater fatigue resistance than nonloaded ulnas, indicating the greater strength in loaded ulnas (and consequent decreased strain per given load) endowed these bones with improved fatigue properties despite their increased mineralization and brittleness.

The current study has strengths, including the use of longitudinal in vivo assessments and the within-animal study of loading effects. These features minimized the total number of animals used and improved statistical power, respectively. The study also has a number of limitations. The mechanical loading model used does not truly represent exercise because it does not require physical exertion on behalf of the animal. However, the strain engendered during forearm axial compressive loading induces bone adaptation in the rat ulna with similar locality and magnitude as observed during physical activities, making the model a useful exercise mimetic (41, 42). The use of relatively low-resolution in vivo pQCT and small size of the

medullary cavity at the ulna midshaft reduced our ability to longitudinally monitor endocortical structural changes. The lifelong maintenance of loading effects may be attributable to species selection, with rodent cortical bone lacking the secondary remodeling of Haversian canals required to remodel and remove excess cortical bone after loading. The current study solely focused on cortical bone, which is minimally responsive to OVX-induced estrogen depletion. It would be informative to perform a similar study at a trabecular-rich skeletal site because the rodent ulna is relatively devoid of trabecular bone and trabecular bone is more susceptible to the skeletal effects of OVX. Finally, the inability to identify interactions between loading and surgery raises the question of whether there was sufficient statistical power to identify such interactive effects between the interventions.

In summary, this study found elevated mechanical loading of the skeleton completed when young had lasting benefits on cortical bone properties that persisted independent of a surgically induced menopause. These findings suggest that skeletal loading associated with exercise when young may provide lifelong benefits to fracture risk by priming the skeleton to offset the cortical bone changes associated with aging and estrogen depletion. Whether these effects translate to humans needs to be shown, but in the interim, individuals should be encouraged to perform load-bearing exercise during skeletal growth to potentiate lifelong bone health.

Acknowledgments

References

1. **Warden SJ.** Extreme skeletal adaptation to mechanical loading. *J Orthop Sports Phys Ther.* 2010;40:188.
2. **Kannus P, Haapasalo H, Sankelo M, Sievänen H, Pasanen M, Heinonen A, Oja P, Vuori I.** Effect of starting age of physical activity on bone mass in the dominant arm of tennis and squash players. *Ann Intern Med.* 1995;123:27–31.
3. **MacKelvie KJ, Khan KM, McKay HA.** Is there a critical period for bone response to weight-bearing exercise in children and adolescents? A systematic review. *Br J Sports Med.* 2002;36:250–257.
4. **Karlsson MK.** Does exercise during growth prevent fractures in later life? *Med Sport Sci.* 2007;51:121–136.
5. **Warden SJ, Fuchs RK.** Exercise and bone health: optimising bone structure during growth is key, but all is not in vain during ageing. *Br J Sports Med.* 2009;43:885–887.
6. **NIH Consensus Development Panel on Osteoporosis Prevention, Diagnosis, and Therapy.** Osteoporosis prevention, diagnosis, and therapy. *JAMA.* 2001;285:785–795.
7. **Rizzoli R, Bianchi ML, Garabédian M, McKay HA, Moreno LA.** Maximizing bone mineral mass gain during growth for the prevention of fractures in the adolescents and the elderly. *Bone.* 2010;46:294–305.
8. **Gunter K, Baxter-Jones AD, Mirwald RL, et al.** Impact exercise increases BMC during growth: an 8-year longitudinal study. *J Bone Miner Res.* 2008;23:986–993.
9. **Honda A, Sogo N, Nagasawa S, Kato T, Umemura Y.** Bones benefits gained by jump training are preserved after detraining in young and adult rats. *J Appl Physiol.* 2008;105:849–853.
10. **Tveit M, Rosengren BE, Nilsson JÅ, Ahlborg HG, Karlsson MK.** Bone mass following physical activity in young years: a mean 39-year prospective controlled study in men. *Osteoporos Int.* 2013;24;1389–1397.
11. **Gustavsson A, Olsson T, Nordström P.** Rapid loss of bone mineral density of the femoral neck after cessation of ice hockey training: a 6-year longitudinal study in males. *J Bone Miner Res.* 2003;18:1964–1969.
12. **Iwamoto J, Yeh JK, Aloia JF.** Effect of deconditioning on cortical and cancellous bone growth in the exercise trained young rats. *J Bone Miner Res.* 2000;15:1842–1849.
13. **Järvinen TL, Pajamäki I, Sievänen H, et al.** Femoral neck response to exercise and subsequent deconditioning in young and adult rats. *J Bone Miner Res.* 2003;18:1292–1299.
14. **Karlsson MK, Linden C, Karlsson C, Johnell O, Obrant K, Seeman E.** Exercise during growth and bone mineral density and fractures in old age. *Lancet.* 2000;355:469–470.
15. **Pajamäki I, Kannus P, Vuohelainen T, Sievänen H, Tuukkanen J, Järvinen M, Järvinen TLN.** The bone gain induced by exercise in puberty is not preserved through a virtually life-long deconditioning: a randomized controlled experimental study in male rats. *J Bone Miner Res.* 2003;18:544–552.
16. **Warden SJ, Fuchs RK, Castillo AB, Nelson IR, Turner CH.** Exercise when young provides lifelong benefits to bone structure and strength. *J Bone Miner Res.* 2007;22:251–259.
17. **Robling AG, Hinant FM, Burr DB, Turner CH.** Improved bone structure and strength after long-term mechanical loading is greatest if loading is separated into short bouts. *J Bone Miner Res.* 2002;17:1545–1554.
18. **Warden SJ, Hurst JA, Sanders MS, Turner CH, Burr DB, Li J.** Bone adaptation to a mechanical loading program significantly increases skeletal fatigue resistance. *J Bone Miner Res.* 2005;20:809–816.
19. **Ahlborg HG, Johnell O, Turner CH, Rannevik G, Karlsson MK.** Bone loss and bone size after menopause. *N Engl J Med.* 2003;349:327–334.
20. **Umemura Y, Nagasawa S, Sogo N, Honda A.** Effects of jump training on bone are preserved after detraining, regardless of estrogen secretion state in rats. *J Appl Physiol.* 2008;104:1116–1120.
21. **Torrance AG, Mosley JR, Suswillo RF, Lanyon LE.** Noninvasive loading of the rat ulna *in vivo* induces a strain-related modeling response uncomplicated by trauma or periosteal pressure. *Calcif Tissue Int.* 1994;54:241–247.
22. **Ström JO, Theodorsson A, Ingberg E, Isaksson IM, Theodorsson E.** Ovariectomy and 17β-estradiol replacement in rats and mice: a visual demonstration. *J Vis Exp.* 2012;e4013.
23. **Doube M, Kłosowski MM, Arganda-Carreras I, et al.** BoneJ: Free

and extensible bone image analysis in ImageJ. *Bone*. 2010;47:1076–1079.

24. **Schriefer JL, Robling AG, Warden SJ, Fournier AJ, Mason J, Turner CH.** A comparison of mechanical properties derived from multiple skeletal sites of mice. *J Biomech*. 2004;38:467–475.

25. **Diez-Perez A, Güerri R, Nogues X, et al.** Microindentation for in vivo measurement of bone tissue mechanical properties in humans. *J Bone Miner Res*. 2010;25:1877–1885.

26. **Gallant MA, Brown DM, Organ JM, Allen MR, Burr DB.** Reference-point indentation correlates with bone toughness assessed using whole-bone traditional mechanical testing. *Bone*. 2013;53:301–305.

27. **Kemp AD, Harding CC, Cabral WA, Marini JC, Wallace JM.** Effects of tissue hydration on nanoscale structural morphology and mechanics of individual type I collagen fibrils in the Brtl mouse model of Osteogenesis Imperfecta. *J Struct Biol*. 2012;180:428–438.

28. **Wallace JM, Chen Q, Fang M, Erickson B, Orr BG, Banaszak Holl MM.** Type I collagen exists as a distribution of nanoscale morphologies in teeth, bones, and tendons. *Langmuir*. 2010;26:7349–7354.

29. **Wallace JM, Erickson B, Les CM, Orr BG, Banaszak Holl MM.** Distribution of type I collagen morphologies in bone: relation to estrogen depletion. *Bone*. 2010;46:1349–1354.

30. **Wallace JM, Orr BG, Marini JC, Holl MM.** Nanoscale morphology of type I collagen is altered in the Brtl mouse model of osteogenesis imperfecta. *J Struct Biol*. 2011;173:146–152.

31. **Durbin PW, Williams MH, Jeung N, Arnold JS.** Development of spontaneous mammary tumors over the life-span of the female Charles River (Sprague-Dawley) rat: the influence of ovariectomy, thyroidectomy, and adrenalectomy-ovariectomy. *Cancer Res*. 1966;26:400–411.

32. **Hotchkiss CE.** Effect of surgical removal of subcutaneous tumors on survival of rats. *J Am Vet Med Assoc*. 1995;206:1575–1579.

33. **Pettersen JC, Morrissey RL, Saunders DR, et al.** A 2-year comparison study of Crl:CD BR and Hsd:Sprague-Dawley SD rats. *Fundam Appl Toxicol*. 1996;33:196–211.

34. **Järvinen TL, Kannus P, Sievänen H.** Have the DXA-based exercise studies seriously underestimated the effects of mechanical loading on bone? *J Bone Miner Res*. 1999;14:1634–1635.

35. **Bagi CM, Mecham M, Weiss J, Miller SC.** Comparative morphometric changes in rat cortical bone following ovariectomy and/or immobilization. *Bone*. 1993;14:877–883.

36. **Barengolts EI, Curry DJ, Bapna MS, Kukreja SC.** Effects of endurance exercise on bone mass and mechanical properties in intact and ovariectomized rats. *J Bone Miner Res*. 1993;8:937–942.

37. **Miller SC, Bowman BM, Miller MA, Bagi CM.** Calcium absorption and osseous organ-, tissue-, and envelope-specific changes following ovariectomy in rats. *Bone*. 1991;12:439–446.

38. **Peng Z, Tuukkanen J, Zhang H, Jämsä T, Väänänen HK.** The mechanical strength of bone in different rat models of experimental osteoporosis. *Bone*. 1994;15:523–532.

39. **Maïmoun L, Brennan-Speranza TC, Rizzoli R, Ammann P.** Effects of ovariectomy on the changes in microarchitecture and material level properties in response to hind leg disuse in female rats. *Bone*. 2012;51:586–591.

40. **Sato M, Zeng GQ, Turner CH.** Biosynthetic human parathyroid hormone (1-34) effects on bone quality in aged ovariectomized rats. *Endocrinology*. 1997;138:4330–4337.

41. **Mosley JR, March BM, Lynch J, Lanyon LE.** Strain magnitude related changes in whole bone architecture in growing rats. *Bone*. 1997;20:191–198.

42. **Welch JM, Weaver CM, Turner CH.** Adaptations to free-fall impact are different in the shafts and bone ends of rat forelimbs. *J Appl Physiol*. 2004;97:1859–1865.

THE ENDOCRINE SOCIETY®

Members can search for endocrinology conferences, meetings and webinars on the **Worldwide Events Calendar.**

www.endo-society.org/calendar